Characterization of Heterojunction Bipolar Phototransistor with Integrated Two-Section Light-Emitting Transistors

Cheng-Han Wu,[1] Yuan-Fu Hsu,[2] Gong-Sheng Cheng,[2] and Chao-Hsin Wu[1,2]

[1]Graduate Institute of Electronics Engineering and [2]Graduate Institute of Photonics and Optoelectronics,
National Taiwan University, No. 1, Sec. 4, Roosevelt Road, Taipei, 10617 Taiwan (R.O.C.)
Phone: +886-2-3366-3694 Email: chaohsinwu@ntu.edu.tw

Keywords: Phototransistor, Light-Emitting Transistor

Abstract

We demonstrated an integrated two-section phototransistor with a light-emitting transistor serving as the light source. The phototransistor optical gain can be modulated by incident optical powers and different bias conditions. With increasing incident optical power, the HPTs absorb more photons and have higher internal gain.

INTRODUCTION

The III-V light-emitting transistor (LET) with direct bandgap and carrier injection has made itself as a three-port (an electrical input, an electrical output and a "third-port" optical output) device. Quantum-wells (QWs), as an optical collector, are incorporated in the *p*-type base layer in order to enhance the base recombination, thus the effective minority carrier lifetime can be progressively reduced to sub-100 ps [1]-[3]. The fast spontaneous recombination lifetime and dual outputs characteristics allow light-emitting transistors to operate as three-terminal high-speed devices and desirable electrical-to-optical converter. Heterojunction phototransistor (HPT) is an attractive component in light wave systems due to its simultaneous photo-detection and amplification in one device, especially in the high speed optical communication systems. The large internal gain, low noise and compatibility with light emitters (e.g. LETs) in epitaxial layer allow the possibility to realize high-performance cost-effective optoelectronic integrated circuits (OEICs) [4]. In the present work, we demonstrate an integrated two-section phototransistor with a light-emitting transistor serving as the light source. We fabricate two InGaP/GaAs LETs with back-to-back orientation (Fig. 1.) and operate one device as light emitter (LET), where the other device as photon-absorption section (HPT). The phototransistor optical gain can be modulated by incident optical powers and different bias conditions. We first demonstrate the phototransistor in a light-emitting transistor platform, i.e. with QWs embedded in the base region of the HPT.

DEVICE STRUCTURE AND FABRICATION

The crystal epitaxial layers in the present work consists (from the GaAs substrate upward) of a 3000 Å *n*-type heavily doped GaAs buffer layer, followed by a 500 Å *n*-type $Al_{0.3}Ga_{0.7}As$ layer, a graded $Al_{0.3}Ga_{0.7}As$ to $Al_{0.9}Ga_{0.1}As$ oxide buffer layer, a 595 Å *n*-type $Al_{0.98}Ga_{0.02}As$ oxidizable layer, and then a graded $Al_{0.9}Ga_{0.1}As$ to $Al_{0.3}Ga_{0.7}As$ oxide buffer layer that completes the bottom cladding layers. These layers are followed by a 557 Å *n*-type subcollector layer, a 120 Å $In_{0.49}Ga_{0.51}P$ etch stop layer, a 2871 Å undoped GaAs collector layer, and a 1358 Å average *p*-doped 3×10^{19} cm^{-3} AlGaAs/GaAs graded base layer (the active layer), which includes among other layers (in the base region) two undoped 112 Å InGaAs QWs (design for $\lambda \approx$ 980 nm). The epitaxial structure is completed with the growth of the upper cladding layers, which consist of a 511 Å *n*-type $In_{0.49}Ga_{0.51}P$ wide-gap emitter layer, a graded $Al_{0.3}Ga_{0.7}As$ to $Al_{0.9}Ga_{0.1}As$ oxide buffer layer, a 595 Å *n*-type $Al_{0.98}Ga_{0.02}As$ oxidizable layer, a graded $Al_{0.9}Ga_{0.1}As$ to $Al_{0.3}Ga_{0.7}As$ oxide buffer layer, and a 500 Å *n*-type $Al_{0.3}Ga_{0.7}As$ layer, a 2000 Å heavily doped *n*-type GaAs contact layer. Finally, the epitaxial structure is capped with a 250 Å $In_{0.49}Ga_{0.51}P$ and a 500 Å GaAs cap layers.

The transistor fabrication is performed by first removing the GaAs cap layer and patterning ~ 800 μm long protective $In_{0.49}Ga_{0.51}P$ stripes. A dilute sulfuric acid solution is used to form the emitter mesa, revealing the $In_{0.49}Ga_{0.51}P$ wide-gap emitter layer. Then, the sample is oxidized at 425 °C in a furnace with N_2 flow mixed with water vapor, resulting in a 4 μm oxide-defined apertures in the 10 μm emitter mesa [5].

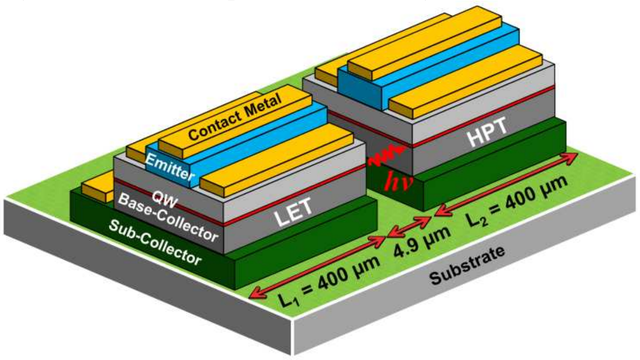

Fig. 1: Schematic device structure of two-section edge-emitting light-emitting transistor where one of them is operated as the light source (LET), and the other one is served as the photodetector (HPT).

A dilute hydrochloric acid solution is used to remove $In_{0.49}Ga_{0.51}P$ layer, exposing the *p*-type GaAs base layer. A Ti/Pt/Au metal is evaporated as *p*-type base contact. The GaAs base and collector layers are removed using selective etch, exposing the heavily doped *n*-type GaAs subcollector layer. An Au-Ge/Ni/Au metal is applied for the emitter and collector ohmic contacts and alloyed at 340 °C. Another sulfuric acid solution is used to isolate devices. A polyimide passivation layer is used for planarization, and a layer of silicon nitride is deposited (~ 1000 Å) using a plasma-enhanced chemical vapor deposition (PECVD) system. Via hole openings are formed by Freon (CF_4) and Oxygen plasma in the reactive ion etching (RIE) to create contact windows to emitter, base, and collector metals. After a contact via fabrication step, a Ti/Au (metal 1 interconnect) is deposited to form contacts from the device to the ground-signal-ground (GSG) probing pads.

In order to form a monolithic two-section device, a thicker silicon nitride is deposited to serve as dry etch mask for inductively coupled plasma reactive ion etching (ICP-RIE) dry etch to form an isolation gap. Finally, another via hole opening is created for electrical probing. The sample is then lapped and mounted on Cu heat sinks, which is temperature controlled by a thermoelectric heater/cooler. Figure 1 shows the schematic device structure of the monolithic two-section edge-emitting light-emitting transistors, where one of them is operated as the light source (LET), and the other one is served as the photodetector (HPT). The lengths of both the LET and HPT are 400 µm. Two devices are separated by 4.9 µm.

COMMON-EMITTER CHARACTERISTICS OF THE HPT WITH OPTICAL INJECTION

Figure 2(a) and 2(b) show the measured common-emitter characteristics for a three-terminal HPT operating in the dark (dash lines) and under 2.25 and 7.16 µW optical injection (solid lines) from the LET serving as a light source under transistor operation. The input base current (I_{Bdc}) flows into the base electrode varies from 0 to 12 mA in 1 mA steps. With the light illumination, the addition holes of photocurrent (I_{ph}) generated from base-collector region inject into the base-emitter junction. It pushes the operating point of the HPT from $I_B = I_{Bdc}$ to $I_B = (I_{Bdc} + I_{ph})$ where the current gain is enhanced. In this situation, the I_{ph} thus constitutes a small signal added to the device's base bias current (I_{Bdc}) and is amplified by the transistor's operation. Addition of I_{ph} to I_{Bdc} is further pushing the operating point of the HPT to higher current where the current gain and hence the optical gain is larger. As a result, the total collector photocurrent $I_{C,opt}$ for a current-bias HPT under optical injection is given by [6]

$$I_{C,opt} = (\beta + 1) I_{ph} + \beta \times I_{Bdc} \tag{1}$$

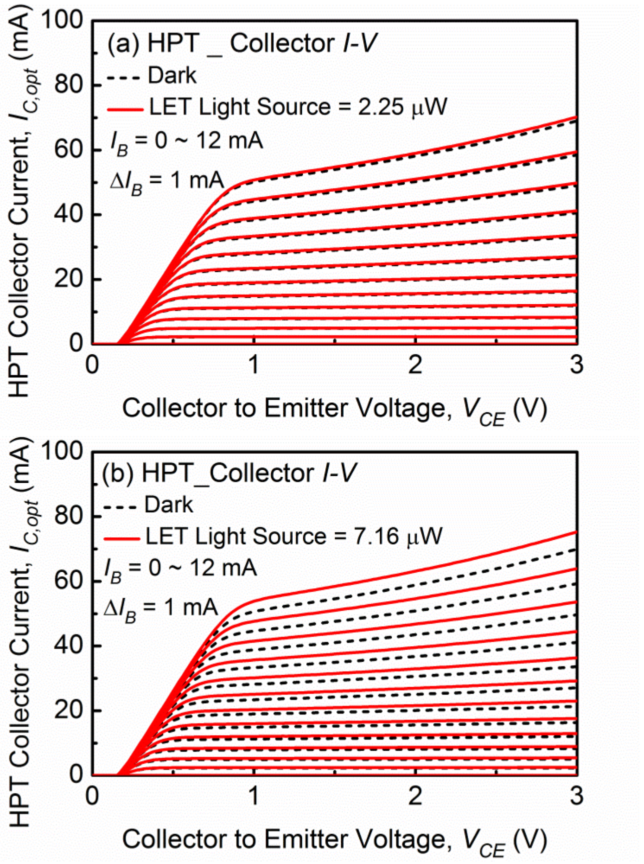

Fig. 2: The common-emitter characteristics of the HPT with incident optical power of (a) 2.25 µW and (b) 7.16 µW respectively.

With the incident input power of 2.25 and 7.16 µW, the total optical collector currents increase 1.8 and 7.6 % respectively at V_{CE} of 3 V and I_B of 12 mA due to the increasing optical absorption. Note that the induced collector photocurrent $\Delta I_{C,opt}$ (i.e. the difference of collector currents between optical injection and dark) is increased with increasing I_{Bdc}. Since the measured β in the dark is increased with increasing base current, Eq. (1) can be employed to explain the enhanced performance of a HPT with a current-injection base.

GUMMEL PLOT OF THE HPT

The Gummel plot is another typical measurement that is also widely employed to characterize the optical/electrical performance of the HPT. In this case, the base-collector voltage is fixed at $V_{BC} = 0$ V, while V_{BE} is changed and the base and collector currents are measured. Figure 3(a) and 3(b) show the base and collector current of the HPT with illumination from LET (circles: 2.25 µW; triangles: 7.16 µW) and without illumination (squares). The reversal I_B shown in Fig. 3(a) with light illumination of 2.25 µW (circles) when $V_{BE} < 0.98$ V arise from the fact that during optical absorption photo-generated holes in the base-collector space charge region are injected into the base exceeding the need

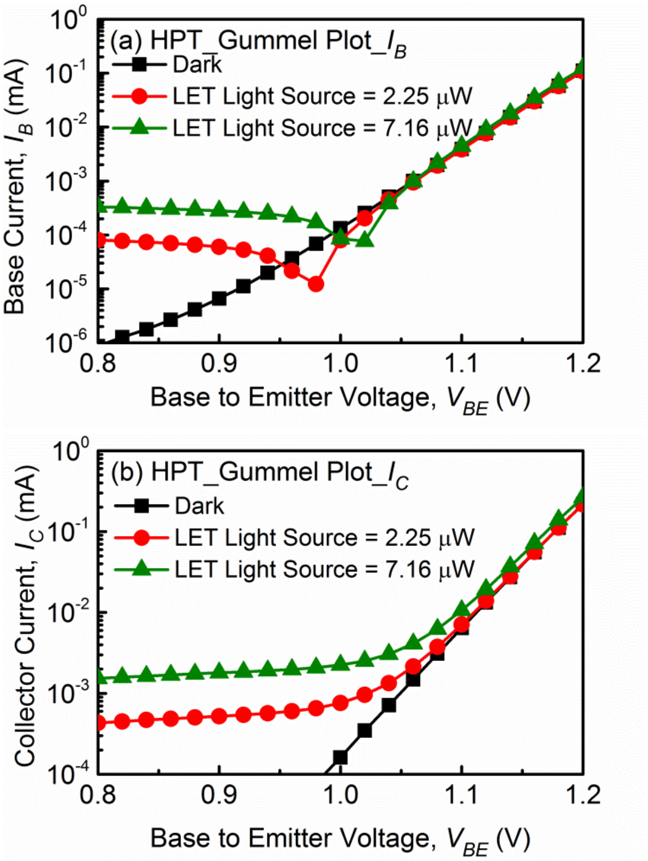

Fig. 3: Gummel plot (a) Base and (b) collector current of the HPT with illumination from LET (●: 2.25 μW; ▲: 7.16 μW) and without illumination (■).

producing a net flow of holes out of the base contact, i.e. a negative base current. At high base-emitter biases (V_{BE} > 1.05 V), the hole injection due to optical absorption is negligible compared to that from the base contact. In this condition, the electrical base current dominates over the photo-generated current leading to coincident curves between illuminated current and dark current. The notches corresponding to the reversal in the base current move to a higher base-emitter bias (0.98 V to 1.02 V) with increasing optical power (2.25 μW to 7.16 μW). At low biases, the base current saturates at a value corresponding to the incident optical power, while the characteristic is unchanged at high biases.. Similarly, Fig. 3(b) shows the collector current's saturation value at low bias shifting to higher current levels with increasing optical power [7].

OPTICAL POWER AND BIAS INFLUENCE ON THE OPTICAL GAIN

Figure 4 shows the device's optical gain as a function of the base currents for a series of different V_{CE} of 1, 2, 3 V and two optical power level injection (P_{in} = 2.25 and 7.16 μW). The optical gain G is calculated from the measured $\Delta I_{C,opt}$ and incident optical power (P_{in}) and given by [8]

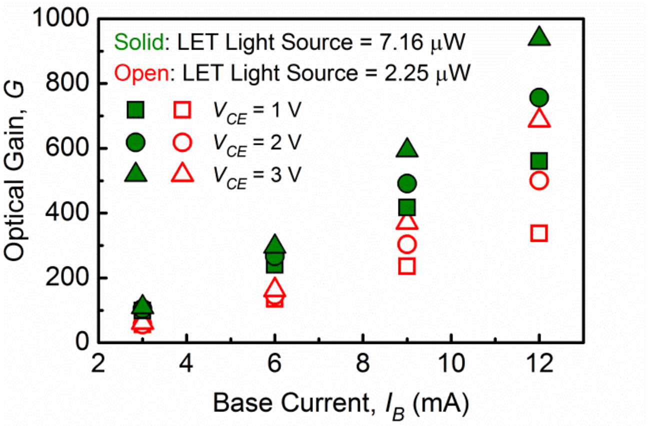

Fig. 4: The optical gain, G, of the HPT with different incident optical powers (P_{in} = 2.25 and 7.16 μW) and biases.

$$G = \frac{h\nu}{q}\frac{\Delta I_{C,opt}}{P_{in}} \tag{2}$$

where ν is the photon's frequency and q is the electronic charge. The optical gain of the HPT increases as the increasing optical power injection. In this case, the optical power takes a role as the base current in the HPT; that is, the optical collector current increases with the input base current. On the other hand, the optical gain at a constant optical power injection is directly proportional to $\Delta I_{C,opt}$. Therefore, we obtain an enhanced optical gain when the HPT is biased with an increasing current source. An optical gain of 940 is obtained when I_B of 12 mA, V_{CE} of 3V and P_{in} of 7.16 μW, which illustrates the advantage of the three-terminal operation of HPT, i.e. the dc base bias can be increased to improve the current and optical gain for a given illumination level. The performance of the HPT employed for the present work is limited by the poor coupling efficiency due to the spontaneous emission of the light source. Further improvement in layout design and process optimization to achieve the laser operation of the LET with high collimated beam will improve the device performance.

CONCLUSIONS

We fabricated a two-section InGaP/GaAs LETs with monolithic back-to-back orientation. One of the devices is operated as a light emitter, and the other one is operated as a phototransistor. The characteristics of HPT have been investigated in this work. The phototransistor optical gain of 940 is achieved under different modulation by incident optical powers and different bias conditions.

REFERENCES

[1] M. Feng, N. Holonyak, Jr., and W. Hafez, *Appl. Phys. Lett.*, **84**, 151, 2004.

[2] M. Feng, N. Holonyak, Jr., and R. Chan, *Appl. Phys. Lett.*, **84**, 1952, 2004.

[3] G. Walter, C. H. Wu, H. W. Then, M. Feng, and N. Holonyak, Jr., *Appl. Phys. Lett.*, **94**, 241101, 2009.

[4] H. Kamitsuna, K. Ishii, T. Shibata, K. Kurishima, M. Ida, *IEEE J. of selected topics in quantum electronics.*, **10**, 673, 2004.

[5] J. M. Dallesasse, N. Holonyak, Jr., A. R. Sugg, T. A. Richard, and N. El-Zein, *Appl. Phys. Lett.* **57**, 2844 s 1990.

[6] S. W. Tan, H. R. Chen, and W. S. Lour, *Appl. Phys. Lett.*, **97**, 034502, 2005.

[7] R. Sridhara, S. M. Frimel, K. P. Roenker, N. Pan, and J. Elliott, *J. Lightwave. Technol.*, **16**, 1101, 1998.

[8] D. C. Scott and H. R. Fetterman, *Indium Phosphide and Related Materials: Processing, Technology and Devices.* Boston, MA: Artech House, 1995, pp. 351–403.

ACRONYMS

LET: Light-Emitting Transistor
QW: Quantum-Well
HPT: Heterojunction Phototransistor
OEICs: Optoelectronic Integrated Circuits
PECVD: Plasma-Enhanced Chemical Vapor Deposition
RIE: Reactive Ion Etching
GSG: Ground-Signal-Ground
ICP: Inductively Coupled Plasma